Orbital degeneracy removed by charge order in triangular antiferromagnet AgNiO$_2$

E. Wawrzyńska[1], R. Coldea[1], E.M. Wheeler[2,3] I.I. Mazin[4], M.D. Johannes[4],

T. Sörgel[5], M. Jansen[5], R.M. Ibberson[6], P.G. Radaelli[6]

[1]*H.H. Wills Physics Laboratory, University of Bristol,*
Tyndall Avenue, Bristol, BS8 1TL, United Kingdom
[2]*Clarendon Laboratory, University of Oxford, Parks Road, Oxford OX1 3PU,*
United Kingdom [3]*Institute Laue-Langevin, BP 156, 38042 Grenoble Cedex 9, France*
[4]*Code 6393, Naval Research Laboratory, Washington, D.C. 20375*
[5]*Max-Planck Institut für Festkörperforschung, Heisenbergstrasse 1, D-70569 Stuttgart, Germany*
[6]*ISIS Facility, Rutherford Appleton Laboratory, Chilton, Didcot OX11 0QX, United Kingdom*
(Dated: February 1, 2008)

We report a high-resolution neutron diffraction study on the orbitally-degenerate spin-1/2 hexagonal metallic antiferromagnet AgNiO$_2$. A structural transition to a tripled unit cell with expanded and contracted NiO$_6$ octahedra indicates $\sqrt{3} \times \sqrt{3}$ charge order on the Ni triangular lattice. This suggests charge order as a possible mechanism of lifting the orbital degeneracy in the presence of charge fluctuations, as an alternative to the more usual Jahn-Teller distortions. A novel magnetic ground state is observed at low temperatures with the electron-rich $S = 1$ Ni sites arranged in alternating ferromagnetic rows on a triangular lattice, surrounded by a honeycomb network of non-magnetic and metallic Ni ions. We also report first-principles band-structure calculations that explain microscopically the origin of these phenomena.

PACS numbers: 75.25.+z, 71.45.Lr

Electronic systems on triangular lattices have attracted wide interest theoretically and experimentally due to the possible existence of unconventional ground states stabilized by the frustrated lattice geometry [1]. The layered cobaltate NaCoO$_2$ with a triangular lattice of orbitally-*non*degenerate Co^{3+} ions [2] shows a number of unusual phases upon hole doping *via* deintercalation of Na, as well as superconductivity upon hydration at a particular doping [1]. The addition of orbital degeneracy creates more instabilities for cooperative order and the behavior in the presence of metallic conductivity is not well understood and largely experimentally unexplored. In more localized systems such as NaNiO$_2$ with spin-1/2 Ni^{3+} ions in the $t_{2g}^6 e_g^1$ configuration the twofold e_g orbital degeneracy is lifted by a Jahn-Teller (JT) structural distortion to a monoclinic structure [3], which splits the e_g band and opens a gap. However it is unclear if such a mechanism applies in less localized systems where the local tendency for JT distortions competes with the charge transfer between sites, allowed by an efficient metallic screening [4]. The metallic layered silver nickelates AgNiO$_2$ [5, 6] and Ag$_2$NiO$_2$ [7] are ideal candidates to explore this physics.

Here we report high-resolution structural studies of AgNiO$_2$ and find that no JT distortions occur but the ideal structure is distorted to a *hexagonal tripled* unit cell with expanded and contracted NiO$_6$ octahedra. This implies that the orbital degeneracy of the formally Ni^{3+} sites is lifted by a novel $\sqrt{3} \times \sqrt{3}$ charge ordering (CO) that occurs via the charge transfer $3e_g^1 \rightarrow e_g^2 + e_g^{0.5} + e_g^{0.5}$, which to the best of our knowledge is the first experimental example of such a CO pattern in a triangular system. Using band-structure calculations we show that

this CO is a 2D analogue of the metal-insulator transition in the 3D RNiO$_3$ [8] attributed to the charge transfer $2e_g^1 \rightarrow e_g^2 + e_g^0$ [4]. However, in contrast to the 3D nickelates in AgNiO$_2$ the triangular lattice geometry allows the system to remain metallic in the CO phase, as itinerant electrons can hop on the inter-connected honeycombe network formed by the two electron-depleted sublattices ($e_g^{0.5}$); those sites remain magnetically unordered at base temperature. The remaining one third of Ni sites are strongly magnetic (e_g^2) and form an effectively tripled antiferromagnetic (AFM) triangular lattice, which orders in an unusual collinear 2×1 structure of alternating stripes.

Powder samples of 2H-AgNiO$_2$ (a polymorph [5] of the better known rhombohedral 3R-polytype [6]) were prepared as described in Ref. [5] and neutron diffraction indicates a nearly pure hexagonal phase with less than 1% admixture of the rhombohedral polytype. Neutron diffraction patterns at 300 K were collected using the high-resolution time-of-flight diffractometers OSIRIS and HRPD at the ISIS pulsed neutron source and representative results are shown in Fig. 1a), yielding the hexagonal space group P6$_3$/mmc as proposed earlier [5], with triangular Ni, O, and Ag layers stacked as ABBBA (Ni-O-Ag-O-Ni). However the neutron data shows additional diffraction peaks [see Fig. 1b)-d)] which can be consistently indexed by an ordering wavevector $\boldsymbol{k}_0 = (1/3, 1/3, 0)$ in the original undistorted structure, indicating a tripled unit cell in the hexagonal plane. To test the accuracy of the indexing we have refined the lattice parameters using only the main peaks and only the supercell peaks (more than 20 observed) and obtained the same values to within the experimental accuracy of 10^{-4} Å. Furthermore, upon cooling to 2 K the super-

cell peaks were displaced in Q following the lattice contraction but maintained their commensurate index with respect to the main peaks. This further confirms that the supercell peaks are due to a modulation of the main structure rather than an extra impurity phase.
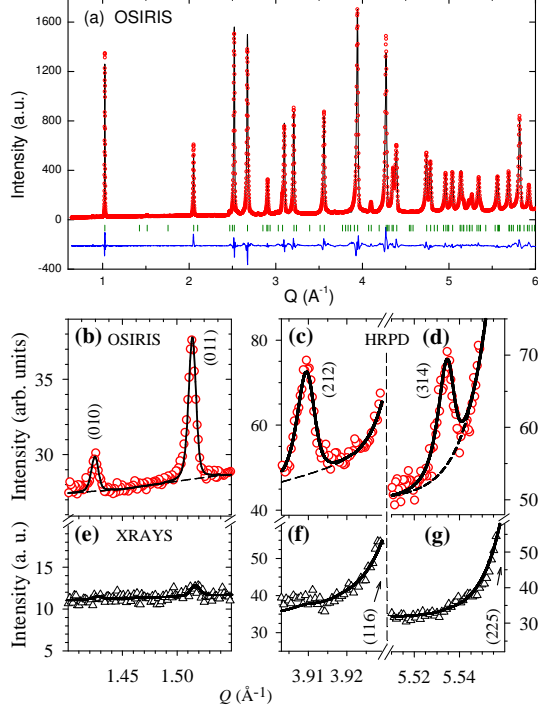

FIG. 1: a) (color online) 300 K neutron powder diffraction pattern and b)-d) zoomed-in regions showing some of the prominent supercell peaks which indicate a distortion of the high-symmetry $P6_3/mmc$ structure where all Ni sites are equivalent. e)-g) Supercell peaks are not observed in xray data indicating that the distortion mainly involves displacements of oxygen ions. Solid lines in all panels are fits to the model with periodic arrangement of expanded and contracted NiO_6 octahedra shown in Fig. 2 and peak indexing is in the triple unit cell (space group $P6_322$).

X-ray data collected using a Phillips Cu K_α powder diffractometer [Fig 1e)-g)] do not show supercell peaks, indicating that the distortion involves mainly the light oxygen ions. Thus we refined the neutron data in a $\sqrt{3} \times \sqrt{3}$ hexagonal unit cell assuming only oxygen displacements. We eliminated the space groups that were not compatible with the observed low-temperature magnetic structure (to be described later) dictating at least two different Ni crystallographic sites. The highest symmetry space group in which both the structural and magnetic data could be described is $P6_322$ (#182). Good agreement with the data is obtained (solid line fits [9] in Fig 1) and the extracted unit cell parameters are listed in Table I. As a further check of the space group identification we have performed full structural optimization calculations (as described later) starting from a lower

TABLE I: Unit cell lattice parameters in the ideal ($P6_3/mmc$) and CO ($P6_322$) structures at 300 K. Internal parameters δ, ζ, ξ, and ϵ are 0, 0.08050(5), 0 and 0.0133(2) (exp.) and 0, 0.0792, 0 and 0.0102 (calc.), respectively.

$P6_3/mmc$ (no. 194)			$P6_322$ (no. 182)		
$a_0 = 2.93919(5)$ Å			$a = 5.0908(1)$ Å		
$c = 12.2498(1)$ Å			$c = 12.2498(1)$ Å		
Atom	Site	(x,y,z)	Atom	Site	(x,y,z)
Ni	$2a$	$(0,0,0)$	Ni1	$2c$	$(\frac{1}{3}, \frac{2}{3}, \frac{1}{4})$
			Ni2	$2b$	$(0, 0, \frac{1}{4})$
			Ni3	$2d$	$(\frac{1}{3}, \frac{2}{3}, \frac{3}{4})$
Ag	$2c$	$(\frac{2}{3}, \frac{1}{3}, \frac{1}{4})$	Ag	$6g$	$(\frac{2}{3} + \delta, 0, 0)$
O	$4f$	$(\frac{2}{3}, \frac{1}{3}, \zeta)$	O	$12i$	$(\frac{1}{3} + \xi, \epsilon, \frac{1}{4} + \zeta)$

symmetry structure ($P6_3$ space group) and those invariably converged to the higher $P6_322$ symmetry, with the optimized positions agreeing well with the experimental ones (Table I) [10].
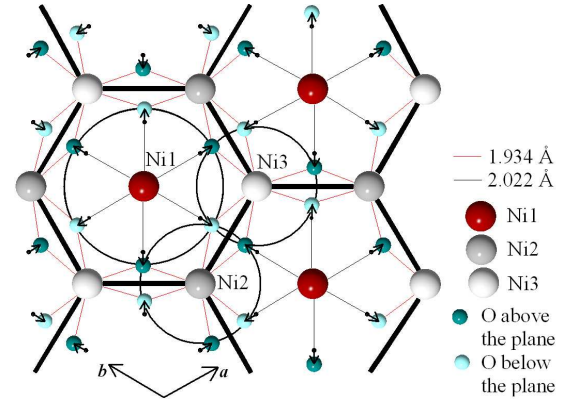

FIG. 2: (color online) Bottom NiO_2 layer showing the expanded $Ni1O_6$ octahedra (large circle) surrounded by a honeycomb network (thick lines) of contracted Ni2 and Ni3 sites (small circles). The small balls are oxygen ions and the small arrows indicate the displacements from the ideal structure.

The resulting structure in one NiO_2 layer is shown in Fig. 2. There are three inequivalent Ni sites. Oxygens breathe in towards Ni2 and Ni3 ions ($d_{Ni2-O} = d_{Ni3-O} = 1.934$ Å) and out from Ni1 ($d_{Ni1-O} = 2.022$ Å). No Jahn-Teller distortion is present. The different Ni-O distances indicate that Ni1 is electron rich (Ni^{2+} in a CO scenario) and Ni2,3 are electron depleted ($Ni^{3.5+}$). In the adjacent NiO_2 layer Ni1 and Ni3 sites swap places, leading to a zigzag arrangement of the (expanded) electron-rich Ni1 sites along c [11].

Earlier susceptibility data [5] showed dominant antiferromagnetic couplings with a Curie-Weiss constant $\theta = -107.6$ K and AFM order below $T_N = 22$ K. Below this temperature additional peaks appear in the neutron
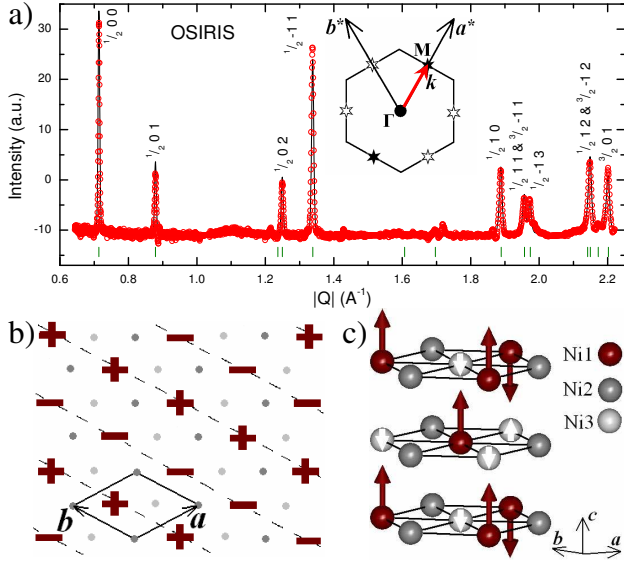
FIG. 3: a) (color online) Magnetic diffraction pattern (difference 4 K - 300 K) indexed by wavevector $\boldsymbol{k} = (1/2, 0, 0)$. Solid line is a fit to the spin order depicted in b): In one layer ordered spins (Ni1) form alternating ferromagnetic rows, $\pm$ symbols indicate spin projection along the c-axis and gray balls are unordered sites (Ni2 and Ni3). Diamond-shaped box is the unit cell. c) 3D view of the magnetic order along c-axis. Band-structure calculations indicate that the effective FM inter-layer coupling between the strongly-magnetic Ni1 spins (large arrows) occurs via AFM couplings to a very small moment at the Ni3 site (small white arrow). Inset in a) shows the 2D hexagonal Brillouin zone with locations of magnetic Bragg peaks (filled stars for the stripe domain in (b), open stars for equivalent domains rotated by $\pm 60°$).

diffraction pattern, see Fig. 3a). These peaks are indexed by the ordering wavevector $\boldsymbol{k} = (1/2, 0, 0)$, as shown in Fig. 3a) inset. The best fit was obtained when only one Ni sublattice was ordered, either Ni1 or Ni3, with a moment of 1.522(7) μ_B along the c-axis. As discussed above, this must be the strongly-magnetic Ni1 (Ni^{2+}) with a large available moment of $S=1$ ($2\mu_B$), because Ni3 and Ni2 are Ni$^{3.5+}$ with only a small available moment.

The observed magnetic structure is shown in Fig. 3b): in each layer ordered spins are arranged in alternating FM stripes, in the adjacent layer stripes are parallel but have an in-plane offset that follows the c-axis zig-zag arrangement of the electron-rich Ni1 sites, see Fig. 3c). This magnetic structure implies that (a) the exchange between nearest in-plane magnetic neighbors is AFM, (b) there is an easy-axis anisotropy $-DS_z^2$, and (c) the net interplanar interaction with the 3 magnetic neighbors in the layer above (below)[see Fig. 3c)] is FM.

To gain more insight into the physical origin for the observed charge and magnetic orderings, we have performed density functional (DFT) calculations [12, 13]. Since Ag$_x$NiO$_2$ is metallic and only weakly correlated[14],

introducing a Hubbard U in the calculation is not necessary. Optimizing the oxygen positions in the $\sqrt{3} \times \sqrt{3}$ unit cell precipitates the CO and reproduces the observed structure in Fig. 2, indicating that the driving force for charge disproportionation is entirely accounted for in the LDA. The calculated total magnetization for the three Ni ions varies between 1.3 and 1.5 μ_B, depending on the exact O position, and is nearly entirely located at the expanded Ni1 site in good quantitative accord with the neutron data. The computed ferromagnetic band structure (Fig. 4) shows fully exchange-split Ni1 derived bands with the magnetic moment diminished from its formal count of 2 μ_B by hybridization. One can also see that Ni2 and Ni3 states are not visibly exchange split. The Ag sp band is entirely above the Fermi level. This electronic structure can be visualized as a magnetic insulator formed by Ni^{2+} (cf. NiO) with a strong tendency to magnetic order, superimposed on a Ni$^{3.5}$ metal. The latter has larger bandwidths, due to the smaller Ni-O distance, and by itself does not satisfy the Stoner criterion for metallic magnetism, $IN(E_F) > 1$, where I is the atomic Stoner parameter.

The natural tendency for charge order in a NiO$_2$ layer can be explained by energetic arguments. The Hund's rule energy gain in a metal in DFT is $M^2(I - N^{-1})/4$, where N is the average density of states per spin. Without charge ordering, $M_1 = M_2 = M_3 = 1\mu_B$ and $N_1 = N_2 = N_3 = \bar{N}$. After charge ordering, $M_1 \approx 2\mu_B$, $M_2 = M_3 \approx 0$ and $N_1 > \bar{N} > N_2 = N_3$. The CO state is energetically favored since $4(I - N_1^{-1})/4 > 3(I - \bar{N}^{-1})/4$. In insulators such as NaNiO$_2$ the Hubbard repulsion would forbid this mechanism, but in this metallic system it is well screened and cannot prevent CO [15]. Our band-structure calculations reproduce fully the observed 3D CO pattern, both the in-plane $\sqrt{3} \times \sqrt{3}$ order as well as the zig-zag arrangement of the electron rich sites along c. We also found a metastable solution where the CO layers form straight columns along c, i.e. the electron rich and strongly magnetic Ni^{2+} occupy the Ni2 site; this indicates that the in-plane CO is very robust and independent of the inter-layer magnetic interactions.

To study the stability of the observed magnetic structure we have calculated ground state energies for a number of potential structures using DFT for the full magnetic unit cell (12 formula units and lower symmetry, C2). In addition to the observed stripe-order with the zig-zag ferromagnetic pattern along c shown in Figs. 3b-c) (called stripe-F), we also found stable solutions for hypothetical ferromagnetic (FM), A-type AFM (alternating FM layers), as well as in-plane stripe-order but with a zig-zag AFM pattern along c (stripe-A, every other plane flipped compared to stripe-F). The results are listed in Table II, the state found experimentally has the lowest energy.

The magnetic structure indicates that the in-plane exchange between magnetic neighbors is AFM. This arises naturally because Ni1^{2+} sites are insulating and lack

TABLE II: Energies of different magnetic configurations for 2H-AgNiO$_2$. All energies are expressed per magnetic Ni1 ion and as a difference from the calculated (and observed) magnetic ground state.

	stripe-F	stripe-A	FM	A-type AFM
Energy/Ni1 (meV)	0	7	23	21

both metallic Stoner ferromagnetism and 90° FM superexchange, but do have a classical AFM superexchange via the Ni1-O-O-Ni1 path, with effective hopping $t_{eff} \sim t_{pd\sigma}^2 t_{pp\pi}/(E_d - E_p)^2$. The appearance of collinear order instead of the conventional 120° order for a triangular AFM implies a significant easy-axis anisotropy. This is normally provided by spin-orbit induced coupling to the crystal field, but the Ni1 ion is close to a $t_{2g}^6 e_g^2$ configuration with zero orbital moment. Further experimental and theoretical studies of the single-site anisotropy in this system are under way. The fact that the effective interplanar Ni1-Ni1 exchange is FM is rather surprising since there is *a priori* no apparent physical mechanism for FM couplings. Indeed, the magnetic species, Ni1, forms insulating bands and Ag is nonmagnetic and absent from the Fermi energy, eliminating double exchange as a possibility. Ni2 and Ni3 form quasi-2D bands with small potential for sizeable RKKY interaction, and magnetic impurities in the Ag layer that could mediate a FM exchange have been excluded experimentally.
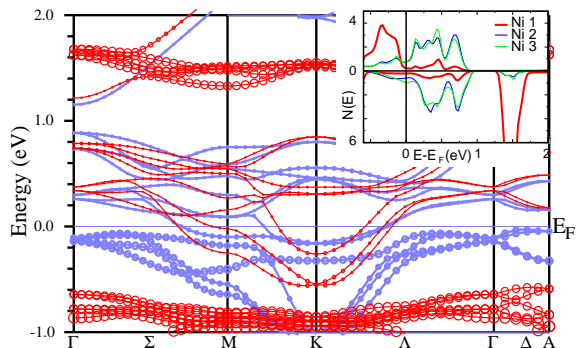

FIG. 4: (color online) Ferromagnetic band structure of 2H-AgNiO$_2$ along symmetry directions in the Brillouin zone. Blue/red (light/dark shades) correspond to the up/down spin directions and circles indicate the relative weight of the Ni1 states. Inset: Partial densities of states for the three Ni sites in states/eV/triple cell. Top/bottom: spin majority (up)/minority(down).

Performing calculations for a wider range of parameters, we find that depending on the exact positions of Ag and O the interplanar interaction can change amplitude and even sign, and that an effective FM interlayer coupling can appear if the weakly-magnetic site Ni3 has a small ordered moment (0.10-0.15 μ_B). The strongest inter-planar interaction is AFM superexchange between the Ni3 and Ni1 directly above (it occurs via a near collinear O-Ag-O path), whereas the inter-planar Ni1-Ni1

exchange is much weaker. If the Ni3 moment is aligned antiparallel to the Ni1 above it then the structure in Fig. 3c) has a net energy gain as it also satisfies two out of the three in-plane AFM Ni3-Ni1 couplings. Our diffraction data in Fig. 3a) cannot prove or exclude the existence of very small moments on Ni3, but the data is consistent with a Ni3 moment of $\sim 0.1\mu_B$ anti-aligned with the Ni1 directly above it, as it comes out of the calculations.

To summarize, we have reported high-resolution neutron diffraction in the orbitally-degenerate 2H-AgNiO$_2$ which observe a periodic arrangement of expanded and contracted NiO$_6$ octahedra, naturally explained by a three-sublattice charge order pattern on the triangular lattice of Ni sites. We have proposed that due to Hund's rule coupling and metallic screening of the Hubbard U repulsion (and static screening due to oxygen displacements) the CO is the favored mechanism to lift the orbital degeneracy as opposed to the conventional Jahn-Teller distortions that occurs in more insulating systems. An unusual magnetic order is observed at low temperatures with only one third of sites carrying a magnetic moment with an unexpected collinear stripe order pattern on an antiferromagnetic triangular lattice. Our results indicate the complex cooperative charge and magnetic order patterns that can occur in orbitally-degenerate metallic systems on frustrated lattices.

[1] N. P. Ong and R. J. Cava, Science **305**, 52 (2004).
[2] M. Jansen and R. Hoppe, Z. Anorg. Allg. Chem. **408**, 104 (1974).
[3] E. Chappel *et al.*, Eur. Phys. J. B **17**, 615 (2000).
[4] I.I. Mazin *et al*, Phys. Rev. Lett. **98**, 176406 (2007).
[5] T. Sörgel and M. Jansen, Z. Anorg. Allg. Chem. **631**, 2970 (2005); J. Solid State Chem. **180**, 8 (2007).
[6] Y.J. Shin *et al.*, J. Solid State Chem. **107**, 303 (1993).
[7] M. Schreyer and M. Jansen, Angew. Chem. **41**, 643 (2002); U. Wedig *et al*, Solid State Sci. **8**, 753 (2006); H. Yoshida *et al*, Phys. Rev. B **73**, 020408(R) (2006).
[8] J.A. Alonso *et al*, Phys. Rev. Lett. **82**, 3871 (1999).
[9] J. Rodríguez-Carvajal, Physica B **192**, 55 (1993).
[10] Experimentally, Ni1-O bond is 4.5% longer than the other two Ni-O, bonds; the calculations find 3.5%. The optimized position of O is mainly insensitive to the position of Ag ions. The Ag ions (located between two O's in the high symmetry structure) do not follow the O ions upon the breathing distortion, remaining instead in a practically ideal triangular lattice. These facts indicate that CO is an intrinsic instability of the NiO$_2$ layer which is only loosely bound to the close-packed Ag layer.
[11] Prominent supercell peaks (Fig. 1b,c) such as (011) and (212) rule out an arrangement where the expanded Ni sites are directly above each other in adjacent layers.
[12] P. Blaha *et al*, WIEN2K, Techn. Universität Wien, Austria, 2001.
[13] G. Kresse and J. Furthmuller, Phys. Rev. B **54**, 11169 (1996).
[14] M. D. Johannes *et al*, Phys. Rev. B (in press 2007).
[15] This analysis does not take into account increase on the Ni-O covalent energy that also favors charge ordering (W.A. Harrison, Phys. Rev. B **74**, 245128 (2006)).